

Design and Simulation of a Solar-Powered EV Charging Station with Battery Backup Using Raspberry Pi Real-Time Monitoring

Pyae Phyo Wai[†], Oghenovo Okpako[†], and Kelvin Anoh[‡]

[†]Department of Energy and Electronic Engineering, University of Portsmouth, United Kingdom

[‡]Centre for Future Technologies, University of Chichester, United Kingdom

Pyae.Wai@myport.ac.uk, oghenovo.okpako@port.ac.uk, k.anoh@chi.ac.uk

Abstract— Electric vehicles (EVs) are increasingly recognized as a key solution to decarbonize the transportation sector, particularly when powered by renewable energy. To support this transition, this study presents the design and simulation of a 4.4 kW off-grid solar-powered EV charging station with integrated battery backup, developed in MATLAB/Simulink. The proposed system operates independently of the utility grid and is evaluated under five environmental and operational scenarios to assess performance and adaptability. The charging station integrates a photovoltaic (PV) array controlled by a Perturb and Observe (P&O) maximum power point tracking (MPPT) algorithm coupled with a boost converter to maximize energy extraction. A diode-based switching mechanism ensures continuous power delivery, either directly from the PV or via the battery. Additionally, a Raspberry Pi module is incorporated for real-time monitoring of the battery's state of charge (SOC), enabling intelligent energy management. Simulation results demonstrate system efficiency ranging from 75% to 95%, with the highest performance observed under standard test conditions. The system remains robust under variable conditions, confirming the viability of off-grid operation. This work contributes a scalable, standalone EV charging solution for locations with limited or no grid access.

Index Terms-Battery Management Systems, Electric Vehicle Charging, Internet of Things, Maximum Power Point Tracking, Photovoltaics, Real-Time Monitoring, State of Charge.

I. INTRODUCTION

The current global challenge of climate change has made decarbonization a necessity. As a result, a concerted effort was made at the United Nations (UN) Paris convention agreement in 2015 by UN members of state to limit global temperature rise to below 2°C and to further pursue an effort to limit it to 1.5°C (UN 2015). The United Kingdom (UK) is a signatory to this agreement and has set a net-zero carbon target by the year 2050 to demonstrate its commitment to the agreement. Transport decarbonisation through adoption of Electric Vehicle (EV) forms a key strategy adopted by the government to achieve to achieve this. According to the UK Committee on Climate Change 6th carbon budget, it is envisaged that there would be surge in EV adoption, driven by the global need to reduce carbon footprint. As a result, the demand for sustainable charging infrastructure becomes very critical [1]. Solar energy

offers a solution to power EV charging stations, reducing reliance on fossil fuel [2]. However, its intermittency due to weather and diurnal cycles poses challenges for consistent charging [3]. Battery storage and advanced energy management are critical for its reliability [4]. Such a system can be deployed off-grid along with a Raspberry Pi communication which offers a real-time monitoring of the battery state of charge. As a result, it becomes important to evaluate the performance of such system under differential environmental conditions.

This study presents an off-grid solar-powered EV charging station with backup battery support, simulated in MATLAB/Simulink. The system includes a 4.4 kW photovoltaic (PV) array, Perturb & Observe (P&O) MPPT algorithm, boost converter, diode-based switching, and coulomb counting for state of charge (SOC) estimation [5][6]. Fig. 1, is a block diagram showing how the system operates.



Fig. 1. Solar powered EV charging system.

It optimizes energy management across diverse conditions, from sunny days to extreme temperatures and zero irradiance, using a 1×10^{-6} s time step simulation to evaluate energy flow, efficiency, and battery performance in five scenarios. Raspberry Pi integration enables real-time monitoring of battery SOC [7][8].

II. METHODOLOGY

A. System Overview

The system model was developed in Simulink and is

presented in Fig. 2. 4.4 kW is delivered from a PV array to charge a 400 V EV battery, with a 400 V backup battery providing supplementary power when needed [8]. Two diodes facilitate automatic switching between power sources based on voltage differentials, eliminating the need for active control. A boost converter steps up the PV output from 40 V to 400 V, and

a priority-based charging logic ensures the EV battery is charged first, with surplus solar power directed to the backup battery. If solar power is insufficient, the backup battery discharges to maintain EV charging [9]. Fig. 2, illustrates the Simulink model, showing the interconnection of subsystems and its implementation.

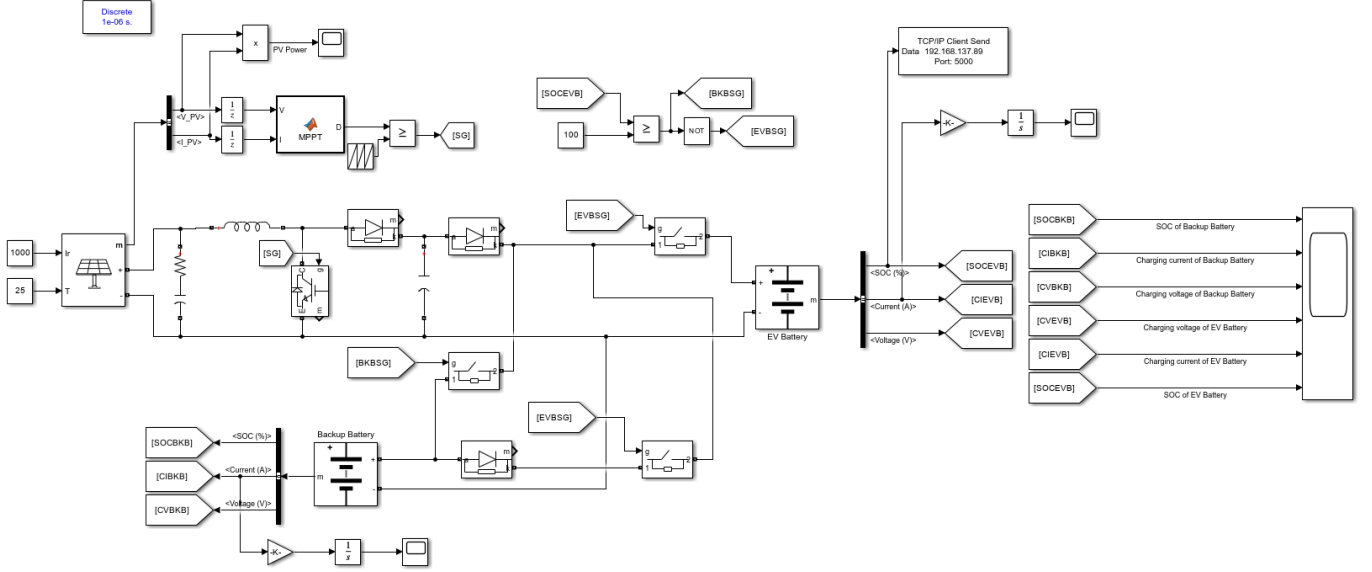


Fig. 2. Simulink model.

B. PV Array Configuration

The PV array consists of parallel strings, each string consists of one module rated at 40 V (voltage at maximum power, V_{mp}) and 11 A (current at maximum power, I_{mp}). The total power output from the solar panel P^{solar} , is calculated using the formula as follows:

$$P^{\text{solar}} = N^m \times V_{mp} \times I_{mp} \quad (1)$$

N^m is the number of modules, which was 10. This configuration ensures operation near the maximum power point, with a safety margin for minor losses [8]. The array is modeled in Simulink to reflect real-world irradiance and temperature variations.

C. MPPT and Boost Converter Design

The Perturb and Observe MPPT algorithm optimizes PV output by adjusting the boost converter's duty cycle (D) to track the maximum power point under varying irradiance and temperature. The algorithm measures PV voltage (V_{PV}) and current (I_{PV}) to compute power ($P = V_{PV} \times I_{PV}$). It perturbs D by a small step ($\Delta D = 0.01$) and observes the power change:

- If $\Delta P > 0$ and $\Delta V > 0$, or $\Delta P < 0$ and $\Delta V < 0$, D increases.
- Otherwise, D decreases.

This iterative process converges to the duty cycle yielding maximum power, typically $D \approx 0.9$ for $V_{PV} = 40$ V and $V_{out} = 400$ V. The algorithm's simplicity ensures effective tracking, though it may oscillate slightly under steady-state conditions [9]. The MPPT is implemented in a Simulink MATLAB function block, processing real-time V_{PV} and I_{PV} inputs.

The boost converter steps up the PV output to 400 V, with the duty cycle calculated as:

$$D = 1 - \frac{V_{mp}}{V_{out}} \quad (2)$$

The converter operates at a switching frequency (f_s) of 50

kHz to balance efficiency and component size. The inductor (L) is sized to limit current ripple ($\Delta I_L = 10\% \times I_{mp} = 10\% \times 11 = 1.1$).

$$L = \frac{(1 - D)V_{in}}{f_{sw}\Delta I_L} \quad (3)$$

A 400 μH inductor is selected to further reduce ripple and enhance stability, accounting for non-ideal conditions [12]. The capacitor (C) minimizes output voltage ripple ($\Delta V_{out} = 1\% \times 400 \text{ V} = 4 \text{ V}$).

$$C = \frac{I_{out}D}{f_{sw}\Delta V_{out}} \quad (4)$$

A 1000 μF capacitor is used to provide a robust energy buffer, reducing ripple and improving transient response [12]. The converter's efficiency is modeled at 95%, with losses due to switching and parasitic resistances [10].

D. Diode-Based Switching Operation

The diode-based switching mechanism ensures seamless power flow in a solar-powered EV charging system, prioritizing EV battery charging and managing backup battery support. Two C4D20120D diodes (1200 V, 20 A, 1.2 V forward drop) direct power from the PV array (via boost converter) or backup battery to the 400 V EV battery bus. The control logic prioritizes solar power for EV charging ($\text{SOC} < 100\%$), engages the backup battery when solar power is insufficient, and redirects surplus solar power to the backup battery at $\text{SOC} = 100\%$ [8]. This passive switching reduces complexity and cost by $\approx 15\%$ compared to MOSFETs [8].

Diode D1 connects the boost converter ($V_{out} \approx 400$ V) to the EV battery bus ($V_{bus} \approx 398\text{--}400$ V), conducting when V_{out} exceeds $V_{bus} + 1.2$ V. Diode D2 connects the backup battery ($V_{backup} \approx 398\text{--}400$ V), conducting when V_{backup} exceeds V_{bus}

+ 1.2 V and solar power is insufficient. Four operational cases include:

- **Sufficient Solar, SOC < 100%:** D1 conducts, $V_{bus} \approx 398.8$ V; D2 is reverse-biased.
- **Insufficient Solar, SOC < 100%:** D2 conducts, $V_{bus} \approx 398.8$ V; D1 is reverse-biased.
- **SOC = 100%, Surplus Solar:** D1 conducts, charging backup battery; D2 is reverse-biased.
- $V_{out} \approx V_{backup}$, **SOC < 100%:** Both diodes may conduct; solar power prioritized.

The diodes offer low losses (5 W per diode, 0.23% of 4.4 kW) and fast recovery (30 ns). Temperature affects forward voltage (1.1 V at 45°C), but the passive design enhances reliability [9]. Limitations include fixed voltage drops and rare current sharing, suggesting Schottky diodes or hybrid switching for future work.

E. Charging Control Method

The charging control shown in Fig. 3, optimizes energy allocation for the solar-powered EV charging system, ensuring efficient use of solar energy and backup battery resources [7].

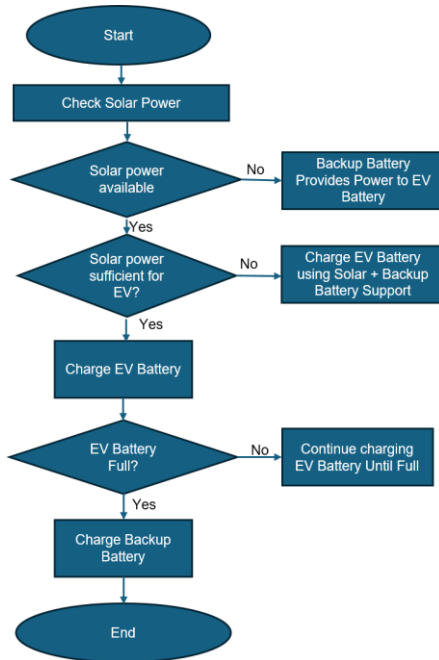


Fig. 3. Charging control.

The control logic prioritizes EV battery charging (SOC < 100%) with solar power, redirects surplus solar energy to the backup battery at SOC = 100%, and engages the backup battery during low solar conditions (e.g., low irradiance) if EV SOC < 100% [7]. Driven by SOC estimation, this strategy ensures continuous charging, minimizes grid reliance, and enhances sustainability [8].

As a Simulink state machine, the control uses conditional blocks to evaluate real-time SOC and power availability [7]:

- **EV Charging (Priority 1):** If EV SOC < 100% and solar power is sufficient, the boost converter delivers $V_{out} \approx 400$ V, D1 conducts, charging the EV battery (8–18 A, 400–440 V) based on SOC and PV output [9].
- **Backup Support (Priority 2):** If solar power is insufficient and EV SOC < 100%, the backup battery

discharges (D2 conducts, $V_{bus} \approx 398.8$ V), with SOC >20% and current (5–10 A) limited [7].

- **Backup Charging (Priority 3):** At EV SOC = 100%, solar power charges the backup battery (D1 conducts, ≤ 4.4 kW), with current capped (≤ 10 A) [8].

Achieving 75–95% efficiency, the control ensures uninterrupted charging [7]. Challenges include SOC estimation reliance and delays during irradiance changes, addressable with predictive algorithms [8]. Future work includes adaptive control for dynamic loads and grid integration [9].

F. Coulomb Counting for SOC Estimation

Accurate SOC estimation is vital for the charging control method, guiding energy allocation [7]. Coulomb counting estimates SOC by integrating net current:

$$SOC(t) = SOC(0) + \left(\frac{1}{C_n}\right) \times \int I(t)dt \quad (5)$$

where SOC (0) is initial SOC, C_n is nominal battery capacity, and $I(t)$ is measured current (positive for charging, negative for discharging) [7]. Implemented in Simulink with a discrete integrator, it updates each time step [10].

With constant C_n , errors are <2% at 25 °C, enabling precise control [9]. At extreme temperatures (-5 °C or 45 °C), errors increase to 5% due to sensor drift and capacity variations [7]. The integrator uses <1% of Simulink’s processing for a 1×10^{-6} s time step [10]. Challenges include drift and current spike sensitivity, addressable with hybrid methods like Kalman filtering [9]. Future work should explore temperature-compensated models and sensor recalibration to achieve <1% error [8].

G. Raspberry Pi Integration

The system’s Raspberry Pi integration shown in Fig. 4, enables real-time SOC monitoring, bridging simulation and practical deployment for enhanced reliability. The Simulink model sends SOC data (32-bit float) to a Raspberry Pi 5 via TCP (port 12345, IP 192.168.1.100), ensuring low-latency transfer. The Raspberry Pi leverages its computational power and IoT connectivity to provide remote access to performance metrics, validating simulations and supporting real-world use.

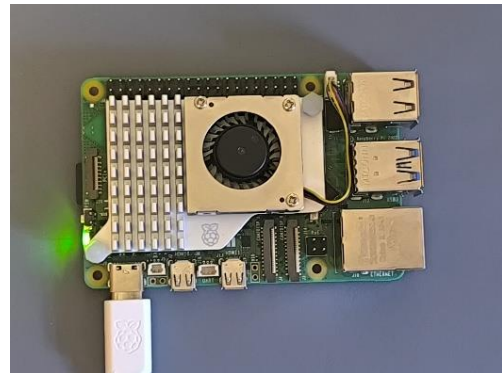


Fig. 4. Raspberry Pi 5.

Raspberry Pi runs a Python-based architecture as follows:

- **main.py:** Manages parallel processes for TCP communication and Blynk cloud updates using multiprocessing for non-blocking operation.

- **TCP_Simulink.py**: Listens on port 12345, unpacks SOC data with `struct.unpack(>f)` for $\pm 0.01\%$ precision, and shares it via a multiprocessing. Queue.
- **Blynk_Interface.py**: Uploads SOC to Blynk's virtual pin (V0) every 1 s, using secure authentication.
- **config.py**: Sets Blynk token, server IP, and retry intervals (e.g., 5 s) for scalability.
- **utils.py**: Logs errors and SOC values to `log.txt` with microsecond precision for debugging.

Blynk's cloud interface displays SOC trends as plots or gauges, enabling remote monitoring. TCP introduces a 10–20 milli seconds (ms) delay, negligible for 1 s updates, and the Pi's 1.5 GHz processor keeps CPU usage $<20\%$. Tested in Simulink over 10 s at 100 Hz, the setup accurately reflects SOC changes. Challenges include network instability, addressed by retries, and minor delays, which could affect real-time control. Future improvements may use MQTT for lower latency or add local storage. Fig. 5, is an EV SOC measurement using Raspberry Pi.



Fig. 5. Blynk Android user interface.

III. SIMULATION SETUP AND SCENARIOS

Five scenarios were designed to test system performance under varying environmental conditions, as summarized in Table I. Each scenario used consistent simulation parameters: a 1×10^{-6} s time step, a 10 s simulation duration, and initial SOC values for the EV and backup batteries. Irradiance and temperature were adjusted to reflect realistic operating conditions, with the discrete solver ensuring high-fidelity data capture despite computational intensity [11].

Table 1. Simulation scenarios.

Scenarios	Solar Irradiance (W/m ²)	Temperature (°C)	Initial EV Battery SOC (%)	Initial Backup Battery SOC (%)
1	1000	25	50	80
2	300	25	20	90
3	1000	45	70	60
4	1000	-5	40	100
5	0	25	10	100

Scenario 1 reflects charging under standard conditions, while Scenario 2 simulates conditions of low sun requiring use of the backup battery. Scenario 3 examines performance on a hot, sunny day, and Scenario 4 addresses a freezing environmental condition where backup battery assistance is needed. Finally, Scenario 5 represents a case with no solar irradiance, in which charging is provided exclusively by the backup battery. The results for all five scenarios are presented and discussed in the following sections.

IV. RESULTS AND DISCUSSION

This section presents the simulation results of a solar-powered off-grid EV charging station with backup battery

support, implemented in MATLAB/Simulink, and discusses their implications. Fig. 6, shows the PV array power output with varying solar irradiance.

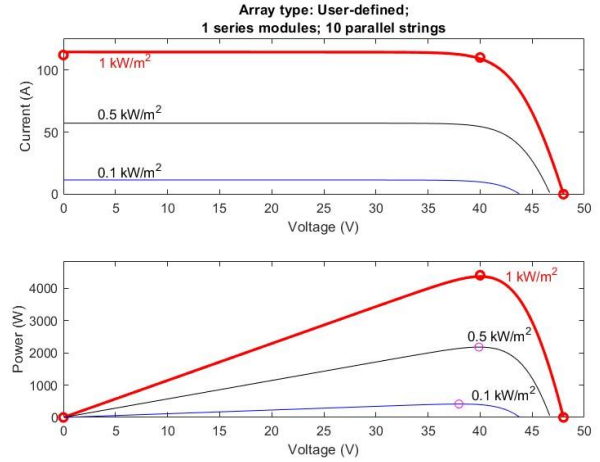


Fig. 6. Solar power output.

As seen in Fig. 6, the PV maximum power increases with increasing solar irradiance. Fig. 7, is the PV power output. Fig. 8, is the charging voltage of EV battery. Fig. 9, is the charging voltage of backup battery. Fig. 10, is the System overall efficiency. They were measured across all five scenarios.

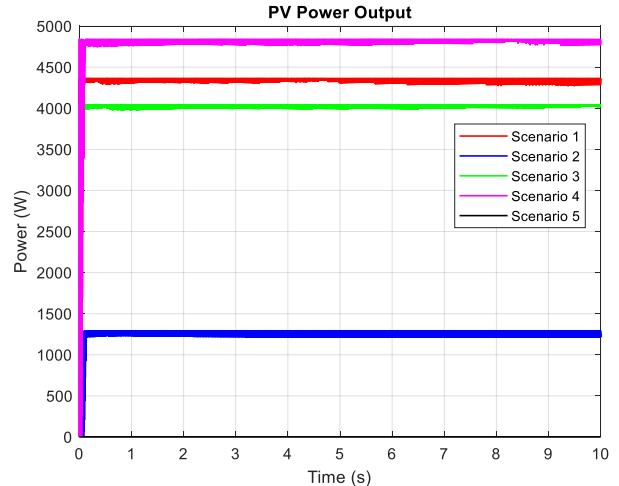


Fig. 7. PV power output across five scenarios.

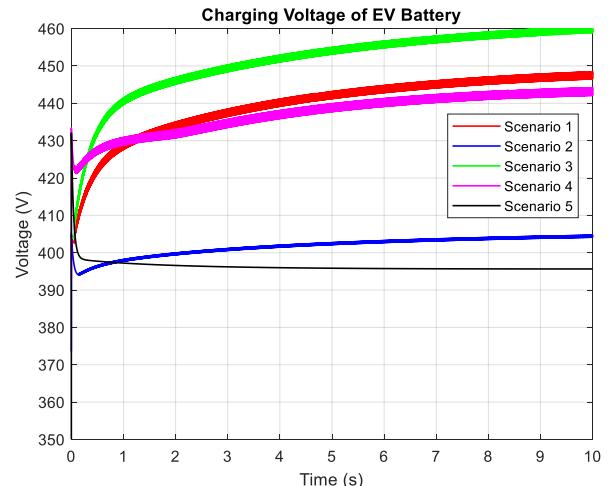


Fig. 8. Charging voltage of EV battery across scenarios.

Under Scenario 1, the PV array delivered a stable 4.4 kW, with the MPPT maintaining a duty cycle of 0.89–0.91. This allowed the EV battery voltage to rise from 400 V to 440 V with a current of 8–13 A, achieving a high system efficiency of 95%. In Scenario 2, the reduced solar input caused PV output to fall to 1.3 kW, necessitating assistance from the backup battery which discharged at 5–10 A and caused system efficiency to decrease to 85%. For Scenario 3 (Hot Day), thermal effects reduced PV output to 4.0 kW consistent with thermal studies [8]; while the EV charged with a current of 7–12 A, efficiency dropped to 90%. Conversely, in Scenario 4 (Freezing Conditions), the PV array's output peaked at 4.8 kW, but the EV's low charge acceptance limited the current to 10–18 A, leading to 20% losses and a system efficiency of just 80%. Finally, in Scenario 5 (No Sun), the system relied entirely on the backup battery, which discharged at 3–5 A to slowly charge the EV, resulting in the lowest efficiency of 75% due to 25% losses in the conversion process.

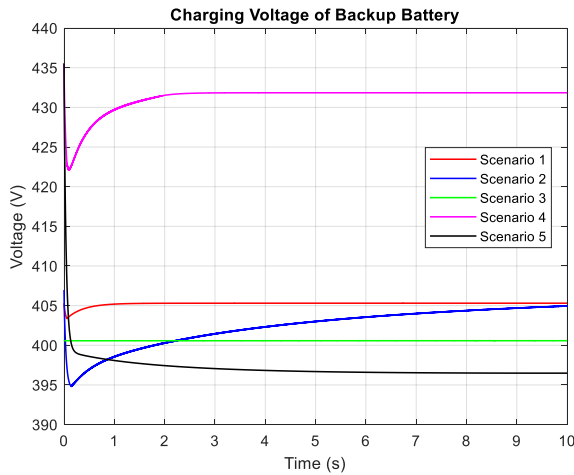


Fig. 9. Charging voltage of backup battery across scenarios.

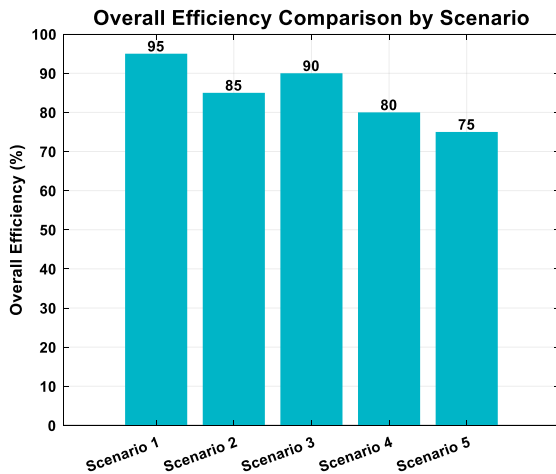


Fig. 10. System overall efficiency across scenarios.

Coulomb counting yielded SOC errors of 2–5%, higher than Kalman filtering, with drift at extreme conditions suggesting hybrid estimation needs. The 1×10^{-6} s time step ensured accuracy but increased computational load, taking hours per simulated second. TCP communication to the Raspberry Pi caused 10–20 ms delays, minor for monitoring but relevant for

real-time control. The integrated approach addresses gaps in component-focused studies. The limitations include steady load assumptions and component discrepancies, as well as challenging hardware translation.

V. CONCLUSION

This study designed an off-grid solar-powered EV charging station with backup battery support. This was simulated in MATLAB/Simulink to evaluate its performance across diverse environmental conditions/scenarios. The novelty lies in integrating real-time electric vehicle battery State-of-Charge (SOC) monitoring via a Raspberry Pi controller with a diode-based power switching network, enabling efficient and autonomous charging operation. Using a 4.4 kW PV array, P&O MPPT, boost converter, diode-based switching, and coulomb counting for SOC estimation, the system achieved 95% efficiency under ideal standard conditions (1000 W/m², 25 °C), with effective EV charging and near-optimal PV operation. Diode switching ensured seamless power flow, and Raspberry Pi integration enabled real-time monitoring. The system adapted to low irradiance, high temperature, freezing conditions, and no solar input/irradiance, and achieved an efficiency of 85%, 90%, 80% and 75% respectively. With the backup battery supporting charging during lower/no solar input, and extreme temperatures further underscoring thermal management needs. The results validate the system's design for sustainable off-grid EV charging and supports scalable infrastructure. Future work should explore dynamic load modeling, advanced thermal management, and hybrid SOC estimation method. Also, optimizing TCP protocols could reduce delays, and hardware validation is needed for diode and MPPT performance.

References

- [1] J. Zhou, Y. Wang, and C. Chen, "Internet of Things (IoT) for renewable energy integration: A review," *Renewable Energy*, vol. 101, pp. 1–7, Feb. 2016.
- [2] V. Salas, E. Olías, A. Barrado, and A. Lázaro, "Review of the maximum power point tracking algorithms for stand-alone photovoltaic systems," *Solar Energy Materials and Solar Cells*, vol. 90, no. 11, pp. 1555–1578, Jul. 2006.
- [3] T. Esram and P. L. Chapman, "Comparison of photovoltaic array maximum power point tracking techniques," *IEEE Trans. Energy Convers.*, vol. 22, no. 2, pp. 439–449, Jun. 2007.
- [4] N. Femia, G. Petrone, G. Spagnuolo, and M. Vitelli, "Optimization of perturb and observe maximum power point tracking method," *IEEE Trans. Power Electron.*, vol. 20, no. 4, pp. 963–973, Jul. 2005.
- [5] A. Pesaran, "Battery thermal management in electric and hybrid vehicles," Argonne National Laboratory, Tech. Rep., 2002.
- [6] MathWorks, "MATLAB and Simulink for engineers," MathWorks Documentation, 2021.
- [7] B. Wu, *High-Power Converters and AC Drives*. Hoboken, NJ, USA: Wiley-IEEE Press, 2006.
- [8] R. W. Erickson and D. Maksimović, *Fundamentals of Power Electronics*, 2nd ed. New York, NY, USA: Springer, 2007.
- [9] J. Zhou, Z. Li, and Y. Zhang, "Energy management systems for solar-powered EV charging stations," *IEEE Trans. Sustain. Energy*, vol. 10, no. 3, pp. 1234–1243, Jul. 2019.
- [10] MathWorks, "Simulink user's guide," MathWorks Documentation, 2021.
- [11] H. Sira-Ramírez and R. Silva-Ortigoza, *Control Design Techniques in Power Electronics Devices*. London, UK: Springer, 2006.
- [12] M. K. Kazimierczuk, *Pulse-width Modulated DC–DC Power Converters*, 2nd ed. Chichester, UK: Wiley, 2014.